

# The magnon BEC observation by switch off method

Yury Bunkov

*Institut Néel, CNRS et Université Joseph Fourier, Grenoble F-38042, France*

*Kazan Federal University, 18 Kremlyovskaja, Kazan 420008, Russia*

E-mail: yuriy.bunkov@grenoble.cnrs.fr

Received January 25, 2017, published online June 26, 2017

The Bose–Einstein condensation (BEC) corresponds to the formation of a collective quantum state in which macroscopic number of particles is governed by a single wave function. The magnon BEC forms by excited non-equilibrium magnons and manifests itself by coherent precession of magnetization even in an inhomogeneous magnetic field. The magnon BEC is very similar to an atomic BEC, but the potential of the interaction between magnons may vary very significantly. The superfluid phases of  $^3\text{He}$  are the best antiferromagnetic system for investigations of magnon BEC and spin superfluidity. The 6 different states of magnon BEC were observed in  $^3\text{He}$ . Recently magnon BEC was observed in antiferromagnets with Suhl–Nakamura interaction and ferrites. Here we review for the first time the switch off NMR method, when magnon BEC forms during a long radiofrequency pulse. The new experimental results are discussed.

PACS: 67.30.H– Superfluid phase of  $^3\text{He}$ ;  
75.10.Kt Quantum spin liquid;  
75.76.+j Spin transport effects;  
76.60.–k Nuclear magnetic resonance.

Keywords: BEC of quasi-particles, non-linear NMR, spin superfluidity, supermagnonics.

## 1. Introduction

The magnetic resonance of magnetically ordered materials is described by magnons, the elementary quanta of excitations of magnetically ordered system with spin equal to 1. In this article we will deal only with magnons with  $k=0$ , which correspond to a homogeneous precession of magnetization. Usually there is a thermal distribution of magnons, which characterized by its temperature. The magnetic resonance corresponds to a creation of new, non-equilibrium magnons. In the case of pulse NMR excited coherent magnons radiate an induction decay signal. But they lose the coherence at a short time, named  $T_2^*$  after the RF pulse due to inhomogeneity of the local conditions. Even for the ferromagnetic and ferrite states the coherence length of exchange interaction is very short and the time of decay signal is very short. Indeed, in some special cases magnons may form non-diagonal long range ordering state which shows all the properties of coherent quantum state. This state corresponds to a Bose–Einstein condensate.

The formation of Bose–Einstein condensed state of bosonic excitations was predicted by Einstein in 1925. The BEC was observed experimentally in dilute gas of cold atoms (in 1995). Earlier (in 1984) [1] the BEC was discov-

ered experimentally for the magnons in superfluid  $^3\text{He-B}$ . The magnon BEC is the spontaneously emerging state of precession of the transverse component of the magnetization, created by RF pumping. This state preserves the phase coherence across the macroscopic volume of the sample even in an inhomogeneous external magnetic field and even in the absence of energy pumping. This is equivalent to the appearance of a coherent superfluid condensate, when all spins precess coherently with the amplitude:

$$M_{\perp} = M_0 \sin \beta, \quad (1)$$

where  $M_0$  — equilibrium magnetization,  $\beta$  — the magnetization deflection angle. This coherent precession is manifested as a huge and long-lived induction signal [1].

The first BEC state of magnons in superfluid  $^3\text{He-B}$  was named Homogeneously Precessing Domain (HPD) [1]. It manifests itself by a region where the magnetization is deflected on a large angle (which corresponds to a «magic» angle of  $104^\circ$ ) and is precessing coherently even in an inhomogeneous magnetic field. The transverse component of magnetization in HPD is described by the wave function  $M_{\perp} e^{i\omega t + \varphi}$ . It possesses all the properties of the spin superfluidity. The spatial gradient of phase  $\varphi$  leads to a spin supercurrent which transports the magnetization. Phase-slip

processes at the critical current [2,3], spin current Josephson effect [4], spin current vortex [5], Goldstone modes [6–8] were observed in superfluid  $^3\text{He-B}$ . The comprehensive review of spin superfluidity in superfluid  $^3\text{He}$  can be found in [9] and recent one in [10–13].

## 2. Magnon BEC versus atomic BEC

The terms of Spin supercurrent and magnon BEC were used by different authors for the different systems. One uses it for a texture of magnetization in a magnetically ordered system. Others use it for describing a magnetic phase transition [14,15]. In the first case the system is stationary and described by a diagonal terms of the density matrix. Non-diagonal terms remain equal to zero. In the second case the system becomes softly unstable towards the growth of one of the magnon modes. The formation of this mode leads to a soft transition to ferromagnetic and/or antiferromagnetic states. This magnetic transition changes the ground state (quantum vacuum) of the system. Again, only diagonal terms of the density matrix rest non-zero. Both of these cases correspond to the equilibrium magnetic states with a chemical potential equal to zero. Contrary the atomic BEC corresponds to a coherent wave function with a correlation of non-diagonal terms of density matrix, the same like in mass superfluidity and superconductivity (see discussion in the book [13]). The magnon BEC, we describe in this article, corresponds to a coherence of non-equilibrium deflected magnetization, that is correlation of non-diagonal terms of density matrix, in a complete analogy with atomic BEC. The coherence of non-diagonal terms directly corresponds to formation of transverse magnetization which precesses and radiates the induction signal. The magnon BEC is formed by a non-equilibrium magnons, which can be pumped by a magnetic resonance. These magnons play the same role as the atoms in the case of classical atomic BEC [16]. The atoms are also excitations of quantum vacuum of our universe, it does not matter that they are very long living excitations. What matters is that the magnons are able to form the BEC state faster than its life time, particularly in superfluid  $^3\text{He}$ . The direct analogy between the magnon and atom BEC formation was analyzed in [17].

The magnon BEC may be formed by pulse or cw NMR. In the first case NMR creates the non-equilibrium magnons. Even being created by a coherent RF pulse, they quickly dephase due to inhomogeneity. Later magnons form spontaneously the state with coherent precession. It was demonstrated at the ideal conditions of pure superfluid  $^3\text{He-B}$ . The timescale of magnon BEC decay is a few orders longer than for the non-coherent case [11]. It means that the magnon BEC state compensates the inhomogeneity of magnetic field by an internal magnon-magnon interaction. The density of magnons decreases with time due to its relaxation (evaporation) and the amplitude of induction

signal decays, but the states remain coherent. Similarly the density of atoms in the BEC state decreases with time due to its evaporation from the trap.

The other method of magnon BEC formation is the applying of a small continuous waves (cw) RF pumping. In this case the external RF field frequency determines the chemical potential for magnon creation. In the conditions of the BEC the density of coherent magnons (the NMR signal) should correspond to a given chemical potential (frequency of pumping) and not to a power of RF pumping [18]. In this case the magnon BEC state is supported by pumping of new magnons. This is possible since the magnons do not thermalize, particularly in the case of superfluid  $^3\text{He}$ . We are able to keep the BEC of excited magnon state permanently, which is not possible for atomic BEC. It is not necessary that the magnon pumping should be coherent — it can be chaotic: the system chooses its own (eigen) frequency of coherent precession, which emphasizes the spontaneous emergence of coherence from chaos. Furthermore, we were able to support permanently the magnon BEC in one cell by exciting the magnons in the other cell connected by a channel of a length about few cm.

And finally the third method, let us say a combined method, the switch off of a long RF pulse. Let us first reconsider the properties of atomic BEC. In this case the atoms are concentrated in a trap that employed both magnetic and optical forces. Evaporation cooling increased the phase-space density by 6 orders of magnitude within seven seconds. Condensates contained up to  $5 \cdot 10^5$  atoms at densities exceeding  $10^{14} \text{ cm}^{-3}$ . “Temperature and total number of atoms were determined using absorption imaging. The atom cloud was imaged either while it was trapped or following a sudden switch-off of the trap and delay time of 6 ms. Such time-of-flight images displayed the velocity distribution of the trapped cloud” [19]. This citation from the Nobel Prize article shows the absolute analogy between the atomic BEC and magnon BEC. In the first case there is the analogy with cw NMR, but at the conditions of relatively short cw NMR pumping. The time-of-flight method is a direct analogy of observation of induction decay signal after switching off the RF pumping. The famous picture from the Nobel lecture of Ketterle [20] Fig. 7 (left side) shows the potato distribution of atoms cloud, cooled to just above the transition point; (middle) just after the condensate appeared and (right) after further evaporative cooling has left an almost pure condensate. There was demonstrated only the records after a 6 ms of time-of-flight. But if one measured the distribution of clouds in other moments of fly, he would see just the analogy with induction decay signal after switching off NMR pumping. The first picture, which shows the potato shape distribution of the atoms, corresponds to a normal thermal distribution of the atoms and to a usual induction decay signal of magnons. The second and third pictures show the slow flying components of atom clouds, which was considered as a proof

of BEC atoms. For magnon system it corresponds to a long living induction decay, which is the decay of BEC state of magnons.

Again, the non-condensed atoms create a wide distribution with the dimensions corresponding to broadening of atomic impulse. In the case of magnon BEC we are able to register the induction decay signal. The non-condensed magnons radiate the usual induction decay signals which decay time corresponds to the inhomogeneity of the magnetic field. Contrary, the coherent magnons create a coherent long lived signal. From this example one can see a similarity of magnon and atomic BEC. Furthermore, the magnon BEC may be prepared by the procedure, very similar to the atomic BEC formation. In the case of atomic BEC, atoms are concentrated in a trap and then are cooled down to the temperature below the critical temperature of the BEC. Similarly, magnons are created in the trap with the temperature below the critical temperature of magnon BEC. The best way of formation of magnon BEC is to pump magnons by a very long but small RF excitation. For usual magnetic systems the induction decay signal is very small or even absent after switching off the long RF pumping. In the case of coherent magnon state, the induction decay signal is very big and long living. That is why the RF switch off method is so important for a magnon BEC observation. Magnon BEC may be formed and observed by a usual short pulse method or by a continuous wave method, but the switch off method is the best for many cases. In the case of HPD in pure  $^3\text{He-B}$  there is no difference between pulse NMR and switch off methods [18].

The magnon BEC has a few advantages in compare with atomic BEC. First of all, the magnon BEC state can be supported by pumping of new magnons. This is possible since the new magnons do not thermalize, particularly in the case of superfluid  $^3\text{He}$ . We are able to keep the magnon BEC state permanently, which is not possible for atomic BEC. It is not necessary that the magnon pumping should be coherent — it can be chaotic: the system chooses its own (eigne) frequency of coherent precession, which emphasizes the spontaneous emergence of coherence from chaos. Second advantage, which is also very important, is the big number of different types of interactions between magnons in different magnetic systems, which leads to many different types of magnon BECs. Up to now we have observed 6 different BEC states in superfluid  $^3\text{He}$  at different conditions [13]. Furthermore the magnon BEC was found in solid antiferromagnets with coupled nuclear-electron precession [21–24] and can be found in many others magnetically ordered materials [25]. Recent investigations shows the possibility of magnon BEC formation in ferrites. We have observed the magnon BEC in Yttrium Iron Garnet film for spin waves with  $\mathbf{k} = 0$ . This magnon BEC differs significantly from the one, observed for big  $\mathbf{k}$  [26]. The preliminary results of this investigations one can found in [27]. All this conditions correspond to a different

quantum vacuum, i.e. magnetically ordered states. In the case of atomic BEC we are deal with only one quantum vacuum of our Universe.

### 3. Magnon BEC in superfluid $^3\text{He}$

The superfluid  $^3\text{He-B}$  is a very perfect quantum vacuum for formation of magnon BEC. The processes of magnetic relaxation are very weak and very well studied [13]. But the interaction between magnons in superfluid  $^3\text{He}$  is very strong, which is manifested by a non-linearity of NMR, a strong dependence of resonance frequency on the density of magnons (chemical potential). The first observed state of magnon BEC (HPD) was formed in a trap, constructed by the gradient of magnetic field and the walls of the experimental cell. The duration of the HPD induction decay may be up to few seconds.

The best analogy with the atomic BEC is demonstrated by a BEC state which is now known as  $Q$ -ball. The  $Q$ -balls are the compact objects — coherently precessing states trapped by orbital texture [28]. If  $N$  magnons are pumped, then the system is similar to the Bose condensate of the ultra-cold atoms in harmonic traps, while at larger  $N$  the analog of the  $Q$ -ball in particle physics is developed [29]. The  $Q$ -ball in superfluid  $^3\text{He-B}$  was discovered by chance as a very strange coherent signal of small amplitude (below 10% of HPD) but extremely long (up to one hour) duration [30]. Later it was found that the frequency of the signal grows up, contrary to the case of HPD [31]. It means that the mechanism of  $Q$ -ball formation is very different from HPD. In the works [32,33] the steady state of  $Q$ -balls have been maintained by cw RF pumping. Again, in contrast with HPD, the signal was excited by sweep field up (frequency down). Finally the signal was explained as a formation of the  $Q$ -ball in a texture trap [29]. It was found that the  $Q$ -ball can be excited even by an off-resonance excitation [28,34]. The recent detailed experimental investigations of  $Q$ -balls formed in the specially prepared and the well controlled traps were made in [35]. The main source of magnons relaxation is the texture of  $^3\text{He-B}$  near the walls of the cell, parallel to a magnetic field [36,37]. The  $Q$ -ball does not touch the walls. That is why it can radiate the induction signal so long as an hour at a frequency of 1 MHz!

### 4. BEC in a systems with impurities

The superfluid  $^3\text{He}$  is an ideal pure system without impurities. The other magnetic systems, particularly solid state magnetically ordered materials, are characterized by a density of different impurities. Therefore, it is very important to study the effect of impurities on the formation of magnon BEC. It is possible to introduce the quasi impurities by immersing the superfluid  $^3\text{He}$  in a very porous material called aerogel. The first experiments with formation of magnon BEC in a systems with impurities gave a very

interesting results. The coherent NMR spectroscopy proved to be extremely useful for the investigation of the superfluid order parameter in this novel system — superfluid  $^3\text{He}$  confined in aerogel [38–42].

Indeed, there is a general problem for the magnon BEC formations in the systems with impurities. If magnons are created by a short RF pulse, its density is redistributed through the sample for creation a single BEC state. For the pure systems, like a superfluid  $^3\text{He-B}$  there is no problem. But in the case of the inhomogeneous distributed impurities the long distance transport of deflected magnetization can be suppressed. As a result the few BEC states are formed in the different places of the sample. In this case the induction decay signal has the beatings between the few signals of BEC states. The signal of BEC for this case is presented schematically in a Fig. 1.

As it was mentioned at Ch. 2, the switch-off NMR technique was developed for improving the observation of BEC formation. In this case, a very long NMR pulse is applied to the sample for creation the BEC. Then we switch-off the RF field and observe the smooth long lived induction decay signal as shown in Fig. 2. Usually, when spins have been pumped for long time, one expects that only those resonating exactly at the pumping frequency will be deflected while all other spins will dephase. However, if a coherent state is excited, all spins in the sample may be deflected and precessing at the same phase and frequency. The observed long lived signal is then the signature of the magnon BEC which decays without loss of coherence. The confirmation of this method was shown in the experiments with superfluid  $^3\text{He-A}$  in aerogel [43,44]. Particularly, relatively short signals have been seen after a short RF pulse. Indeed, it was significantly longer than the signal from non-BEC magnons at the same sample. After a long signal one was able to see the very long living signal. Indeed the starting amplitude was about the same as after a short pulses (see Fig. 3 in the article [43]).

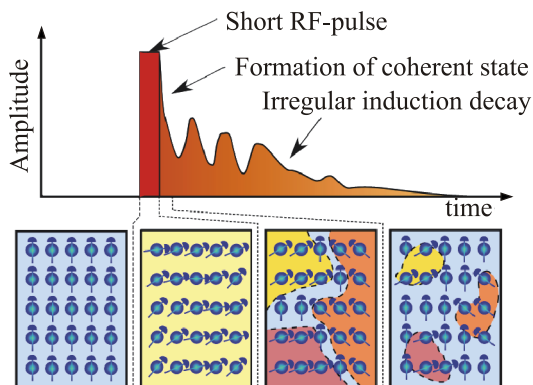


Fig. 1. The scheme of BEC formation after a short NMR pulse. The magnons are condensed in a different parts of the sample owing to the inhomogeneity of the aerogel. The induction signal shows the beating between different BEC states.

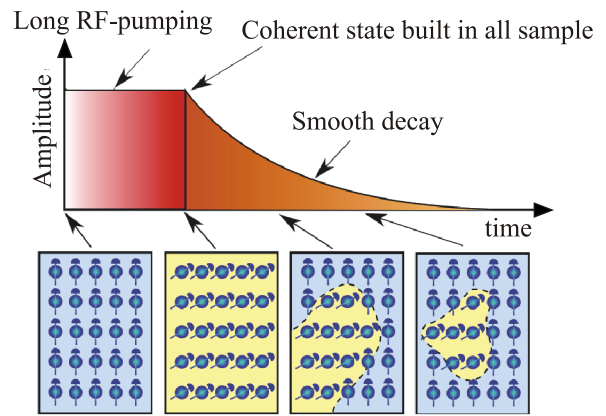


Fig. 2. The scheme of BEC formation after a long NMR pulse. During the pulse the magnons are condensed on a single BEC state. After the switch off the RF power the BEC state radiate a smooth induction signal, which is relaxing but remains coherent.

### 5. Magnon BEC in antiferromagnets

The most remarkable property of the antiferromagnets with Suhl–Nakamura interaction is the coupled nuclear–electron precession of two completely different magnetic subsystems. Electron spins are ordered by an exchange interaction while the nuclear spins are in the paramagnetic state. Due to coupling through the hyperfine field, the frequencies of magnetic resonance are changed. The frequency of the electron magnons increases, while the nuclear magnetic resonance frequency decreases and becomes significantly lower than the Larmor frequency of the nuclear spins. Let us mark the low frequency quasi NMR mode as nuclear–electron magnetic resonance (NEMR) mode and high frequency quasi antiferromagnetic resonance mode as electron–nuclear magnetic resonance (ENMR) mode. The properties of magnetic subsystems change significantly due to the coupled precession. The hyperfine gap appears in the spectrum of antiferromagnetic spin waves. The quasineuclear spin waves appear, with the antiferromagnetic length of coherence. In other words, the nuclear magnetic system gets some properties of magnetically ordered system due to involvement of electron subsystem. In a good approximation, the non-shifted frequencies of the nuclear and electron resonances  $\omega^{n0}$  and  $\omega^{e0}$  and the shifted frequencies  $\omega^n$  and  $\omega^e$  can be described by the following relation

$$\omega^{n0}\omega^{e0} = \omega^n\omega^e. \quad (2)$$

The energy of interaction between the nuclear and electron branches is determined by the hyperfine field resulting from the nuclei acting on the electrons

$$H_{hf}^e = A\gamma_e m_z = A\gamma_e m_0 \cos\beta, \quad (3)$$

where  $m_z$  is the projection of the nuclear magnetization on the electron magnetization, which is controlled by the nuclear

magnetization  $m_0$  and may be reduced by heating or by deflecting the angle  $\beta$ . In the latter case, we may speak about an interesting non-linear phenomenon, i.e., the frequency dependence of the spin excitation, as was theoretically discussed by de Gennes *et al.* [45]:

$$\omega^n = \omega^{n0} - \omega_{p0} \cos\beta. \quad (4)$$

This dynamical frequency shift of the nuclear magnetic resonance, caused by the so-called «pulling» effect, possesses many similar properties with the frequency shift in superfluid  $^3\text{He-A}$ : The NMR frequency depends strongly on the deflection angle of the magnetization. For the  $\text{CsMnF}_3$  and  $\text{MnCO}_3$  antiferromagnets the nuclear magnetic resonance (NMR) frequency  $\omega^{n0}$  of  $^{55}\text{Mn}$  is very high, being about 600 MHz, while the electron AFM resonance (AFMR) frequency  $\omega^{e0}$  might be very low at small external magnetic fields  $H$ . The frequency shift  $\omega_{p0}$  may be so big as hundreds of MHz!

The dynamic properties of coupled nuclear–electron precession in a considered antiferromagnets are very similar to a  $^3\text{He-A}$  in aerogel [24]. That is why we have made a search of magnon BEC signals in these antiferromagnets. It is very important to mention, that the magnon–magnon interaction for the ENMR mode is attractive, while for NEMR mode is repulsive. Consequently the BEC state formation is not possible for the first case and possible for the second case. And particularly, the BEC state was observed for NEMR mode [21]. Furthermore, the magnetic relaxation of nuclear magnons does not describes by Bloch equations, but by Landau–Lifshitz equations due to a strong interaction with magnetically ordered electron state [25].

### 6. Minimization of free energy

As in the case of the atomic BEC the essential physical picture of the magnon BEC can be described by the Ginzburg–Landau free energy functional  $F$  which (in the reference frame rotating with the RF frequency  $\omega_{RF}$ ) is given by [10]:

$$\mathcal{F} = \int d^3r \left\{ \frac{|\nabla\Psi|^2}{2m_M} + [\omega_k^n - \omega_{RF}] |\Psi|^2 + \frac{b}{2} |\Psi|^4 \right\}. \quad (5)$$

For magnon systems the complex order parameter  $\Psi(r, t)$  is the vacuum expectation value of the magnon field operator  $\hat{\Psi}(r, t)$ :  $\Psi(r, t) = \langle \hat{\Psi}(r, t) \rangle$ . For homogeneous precession the magnon number density  $n$  can be related to the deflection angle  $\beta$  via  $n = |\Psi|^2 = m(1 - \cos\beta)$ . The first term in the Eq. (4) describes the kinetic energy of magnons with the effective mass  $m_M = 2/\omega_{p0}^2$ . The resonance frequency of homogeneous ( $k = 0$ ), low amplitude ( $\beta = 0$ ) NMR:  $\omega_k^n \equiv \omega_k^n(0, 0) = \omega^{n0} - \omega_p(0)$ , plays the role of an external potential in atomic condensates. The last term with  $b = \omega_p/m$ , originating from  $\beta$ -dependence of  $\omega_p(\beta)$

describes the dynamical frequency shift up and, within Eq. (4), can be interpreted as a self-similar non-linear contribution to the potential energy of magnons due to their repulsion.

The atomic BEC forms in a trap, which is usually a trap of potential energy. The same type of trap used for  $Q$ -ball in superfluid  $^3\text{He-B}$  at very low temperatures, where the trap formed by spatial texture and by minimum of magnetic field [35]. The trap for HPD formed simultaneously by inhomogeneity of magnetic field, walls of the cell and dipole-dipole energy [10]. In the case of  $^3\text{He-A}$  in aerogel and considered here antiferromagnets the traps formed only by the energy of interaction. Let us calculate the Ginzburg–Landau free energy (Eq. (5)) for the conditions of real experiment, we will consider here. The potential for this conditions is shown in Fig. 3. One can clearly see the minimum of potential. This minimum is reached at  $\nabla\Psi = 0$  (i.e., for homogeneous excitation–magnons with  $k = 0$ ) and for  $b|\Psi|^2 = \omega_{RF} - \omega_k^n$ . This can be identically rewritten as condition of homogeneous nonlinear NMR:

$$\omega_{RF} = \omega_0^n(\beta) = \omega^{n0} - \omega_p(0) \cos\beta. \quad (6)$$

It means that the magnetization of all the sample may condensed in the state, corresponds to minima of potential at the angle  $\beta 18^\circ$  at the conditions of Fig. 3. It is very important to note that in the case of inhomogeneity of  $\omega^n$  the minimum of potential would appear for a slightly different angle of deflection. In other words the inhomogeneity of local field can be compensated by Suhl–Nakamura interaction and all the magnetic moments would rotate at the same frequency all over the sample. In this case, after switching off the NMR pumping the spin system should radiate a big and very long living induction decay signal.

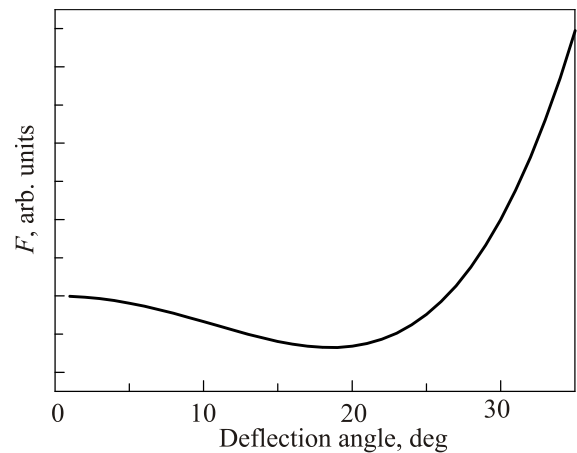


Fig. 3. The profile of Ginzburg–Landau potential in  $\text{CsMnF}_3$  at a frame rotating with the frequency of RF pumping. The parameters are:  $\omega_{RF}/2\pi = 562$  MHz,  $\omega_0^n/2\pi = 554.8$  MHz.

## 7. Switch-off NMR in antiferromagnets

The switch-off method plays a crucial role for the magnon BEC investigations in antiferromagnets with Suhl–Nakamura interaction. The experiment was performed on  $\text{CsMnF}_3$  at the temperature of 1.5 K and RF frequency of about 562 MHz. We have applied the external magnetic field at which the induction decay signal with maximal amplitude was observed after a very short but intensive RF pulse. It corresponds to shift of about 2 MHz of the RF pumping frequency from the resonance frequency at given magnetic field. The signal is shown in Fig. 4. From the induction decay signal we can estimate the inhomogeneity of the NMR line, which characterized by decay time constant  $T_2^*$ . Furthermore, we have applied the sequence of two pulses with time delay and observed the spin echo signal. By this method we were able to measure the  $T_2$  of the system at our experimental conditions, which is about 1.4  $\mu\text{s}$ . As a result, we know all main parameters of linear NMR signal. Now let us change the experimental conditions for the observation of BEC of magnons. For this purpose we have changed the magnetic field which corresponds to resonance at a frequency 554.8 MHz. The RF frequency remains the same meaning the increasing of frequency shift  $\Delta\omega = \omega_{RF} - \omega_0^n(0)$  up to 7.2 MHz. This frequency shift provides the deflection angle of about  $\beta \approx 18^\circ$  according to Eq. (6). Then we have applied a long RF pulse. We observed a very long induction decay signal (Fig. 4) with the intensity comparable to the intensity after a short pulse. We have varied the length of the pulse and the amplitude of excitation. The signal amplitude does not depend on the length and intensity of the RF pulse starting from some critical conditions (RF power is more than 40 mW and the pulse length is more than 100 ms [46]) but corresponds well to the condition (1) of magnon BEC. What is very important to mention is that the length of the induction signal is even longer than the transverse relaxation time  $T_2$  measured after a short pulse!

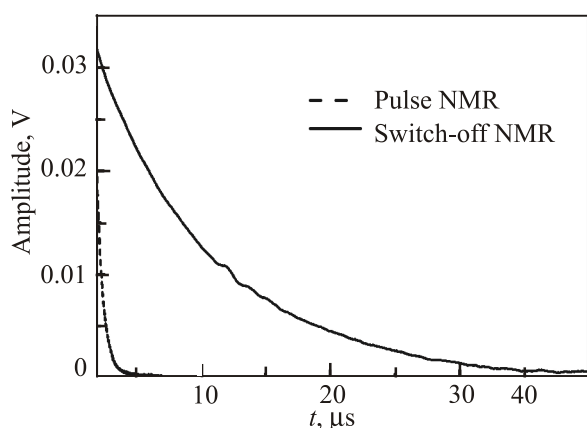


Fig. 4. The free induction decay in  $\text{CsMnF}_3$  after a short RF pulse (pulse NMR technique) and after a long RF pulse (switch-off technique).

## 8. Conclusion

In this article we described the application of a switch off method of magnetic resonance for creation of magnon BEC in the samples with a big concentration of impurities. The method was used early for an observation of a long induction decay signals in superfluid  $^3\text{He-A}$  [43] and  $\text{CsMnF}_3$  [22]. This method is the best for demonstration of the formation of magnon BEC in the antiferromagnets with Suhl–Nakamura interaction. The magnon BEC formed during the long pulse. The magnons condensed to the minimum of Ginzburg–Landau potential and are described by a single wave function with a fixed phase and frequency. Usually there is an inhomogeneity of local NMR Larmor frequency on the sample. This inhomogeneity is compensated by the small local variation of angle  $\beta$ . That is by the density of magnons. At the moment of switch off the RF pumping the magnons remain at the same state for a long time and demonstrate the coherence of precession even at the inhomogeneity of local conditions. We have found that the length of the BEC induction signal is even longer than the characteristic time of spin-spin relaxation  $T_2$ .

Let us now show that the experimental results clearly demonstrates the formation of magnon BEC in  $\text{CsMnF}_3$ .

1. First of all the amplitude of induction decay of magnon BEC is significantly bigger than the amplitude of a signal after a short resonance pulse [22]. From point of view of usual magnetic resonance the amplitude should decrease with the increasing of the length of the pulse owing the relaxation in a rotating frame. After a very long pulse the induction decay signal should vanish.

2. The amplitude of BEC signal does not depends on the amplitude of RF field [22] in agreement with the theory of magnon BEC! In the case of usual NMR a small induction signal may appears at the moment of switch off. This signal should linearly increase with increasing of RF field.

3. The amplitude of BEC signal grows with increase of frequency shift of RF field from the Larmor frequency [22] in a perfect agreement with the BEC theory. The signal should decrease with the frequency shift if it is due to heating of spin system, as was suggested in early publications [47,48].

4. There were observed a very long induction decay signals, an order of magnitude longer then the reverse inhomogeneity of magnetic field, which determines the length of the signal in usual case. Someone can say that the long pulse may excite only the narrow part of the spectrum of magnons, which may decay longer. Indeed, the signal should not be longer than the  $T_2$ . The length of BEC signal is significantly longer then  $T_2$ , as shown in this article.

5. And finally, the formation of magnon BEC was clearly demonstrated in superfluid  $^3\text{He-A}$ . Particularly the amplitude of BEC signal was well calibrated by the signal in  $^3\text{He-B}$  [44]. To make calibration of the BEC signal in  $\text{CsMnF}_3$  is difficult. Indeed, the non-linear spin

dynamics of nuclear branch of magnetic resonance in CsMnF<sub>3</sub> is very similar. And the experimental results, we have observed, corresponds one to one to a results of BEC in <sup>3</sup>He–A.

The new method of magnetic resonance, the switch off method is very appropriate for the investigations of magnon BEC. This method is very similar to one, used for atomic BEC formation. This method excludes the transient processes of BEC formation which can violate a BEC formation in the case of pulsed magnetic resonance. It is also favorable in comparison with cw resonance method. In the latter case the signal of the BEC mixed with the signal of RF pumping. Finally, the switch off method is most favorable for the case of solid magnetic materials, which are characterized by a high density of impurities and high level of local inhomogeneity.

### Acknowledgements

The author thanks to a discussions with my colleges in the laboratory of non-linear magnetic resonance and spin superfluidity of Kazan Federal University and in Ultra Low Temperature group of the Institute Neel, Grenoble, France. This work was financially supported by the Russian Science Foundation (grant RSF 16-12-10359).

1. A.S. Borovik-Romanov, Yu.M. Bunkov, V.V. Dmitriev, and Yu.M. Mukharskiy, *JETP Lett.* **40**, 1033 (1984).
2. A.S. Borovik-Romanov, Yu.M. Bunkov, V.V. Dmitriev, and Yu.M. Mukharskiy, *JETP Lett.* **45**, 124 (1987).
3. A.S. Borovik-Romanov, Yu.M. Bunkov, V.V. Dmitriev, Yu.M. Mukharskiy, and D.A. Sergatskov, *Phys. Rev. Lett.* **62**, 1631 (1989).
4. A.S. Borovik-Romanov, Yu.M. Bunkov, A. de Waard, V.V. Dmitriev, V. Makroczyova, Yu.M. Mukharskiy, and D.A. Sergatskov, *JETP Lett.* **47**, 478 (1988).
5. A.S. Borovik-Romanov, Yu.M. Bunkov, V.V. Dmitriev, Yu.M. Mukharskiy, and D.A. Sergatskov, *Physica B* **165**, 649 (1990).
6. Yu.M. Bunkov, V.V. Dmitriev, and Yu.M. Mukharskiy, *JETP Lett.* **43**, 168 (1986).
7. Yu.M. Bunkov, V.V. Dmitriev, and Yu.M. Mukharskiy, *Physica B* **178**, 196 (1992).
8. M. Kupka and P. Skyba, *Phys. Rev. B* **85**, 184529 (2012).
9. Yu.M. Bunkov, *Spin Supercurrent and Novel Properties of NMR in <sup>3</sup>He*, *Prog. Low Temp. Phys.* **14**, 69, W. Halperin (ed.), Elsevier, Amsterdam (1995).
10. Yu.M. Bunkov and G.E. Volovik, *J. Low Temp. Phys.* **150**, 135 (2008).
11. Yu.M. Bunkov and G.E. Volovik, *J. Phys.: Condens. Matter* **22**, 164210 (2010).
12. Yu.M. Bunkov, *J. Phys.: Condens. Matter* **21**, 164201 (2009).
13. Yu.M. Bunkov and G.E. Volovik, *Spin Superfluidity and Magnon BEC (Novel Superfluids)*, K.H. Bennemann and J.B. Ketterson (eds.), University press, Oxford (2013).
14. T. Giamarchi, Ch. Rüegg, and O. Tchernyshyov, *Nature Phys.* **4**, 198 (2008).
15. S.N. Kaul and S.P. Mathew, *Phys. Rev. Lett.* **106**, 247204 (2011).
16. L. Pitaevskii and S. Stringari, *Bose–Einstein Condensation*, Clarendon Press, Oxford (2003).
17. Yury Bunkov, *J. Low Temp. Phys.* **183**, 399 (2016).
18. A.S. Borovik-Romanov, Yu.M. Bunkov, V.V. Dmitriev, Yu.M. Mukharskiy, E.V. Poddyakova, and O.D. Timofeevskaya, *Sov. Phys. JETP* **69**, 542 (1989).
19. K.B. Davis, M.O. Mewes, M.R. Andrews, N.J. van Druten, D.S. Durfee, D.M. Kurn, and W. Ketterle, *Phys. Rev. Lett.* **75**, 3969 (1995).
20. Wolfgang Ketterle, [http://www.nobelprize.org/nobel\\_prizes/physics/laureates/2001/ketterle-lecture.pdf](http://www.nobelprize.org/nobel_prizes/physics/laureates/2001/ketterle-lecture.pdf).
21. Yu.M. Bunkov, E.M. Alakshin, R.R. Gazizulin, A.V. Klochkov, V.V. Kuzmin, T.R. Safin, and M.S. Tagirov, *JETP Lett.* **94**, 68 (2011).
22. Yu.M. Bunkov, E.M. Alakshin, R.R. Gazizulin, A.V. Klochkov, V.V. Kuzmin, V.S. L'vov, and M.S. Tagirov, *Phys. Rev. Lett.* **108**, 177002 (2012).
23. E.M. Alakshin, Yu.M. Bunkov, R.R. Gazizulin, A.V. Klochkov, V.V. Kuzmin, R.M. Rakhmatullin, A.M. Sabitova, T.R. Safin, and M.S. Tagirov, *Appl. Mag. Reson.* **44**, 595 (2013).
24. Yu.M. Bunkov, *Phys. Usp.* **53**, 843 (2010).
25. M.A. Borich, Yu.M. Bunkov, M.I. Kurkin, and A.P. Tankeev, *JETP Lett.* **105**, 23 (2017).
26. D.A. Bozhko, P. Clausen, G.A. Melkov, V.S. L'vov, A. Pomyalov, V.I. Vasyuchka, A.V. Chumak, B. Hillebrands, and A.A. Serga, *Nature Phys.* **12**, 1057 (2016).
27. Yu.M. Bunkov, P.M. Vetoshko, I.G. Motygullin, T.R. Safin, M.S. Tagirov, and N.A. Tukmakova, *Magn. Res. Solids* **17**, 12502 (2015).
28. Yu.M. Bunkov, *J. Low Temp. Phys.* **138**, 753 (2005).
29. Yu.M. Bunkov and G.E. Volovik, *Phys. Rev. Lett.* **98**, 265302 (2007).
30. Yu.M. Bunkov, S.N. Fisher, A.M. Guenault, and G.R. Pickett, *Phys. Rev. Lett.* **69**, 3092 (1992).
31. Yu.M. Bunkov, S.N. Fisher, A.M. Guenault, G.R. Pickett, and S.R. Zakazov, *Physica B* **194**, 827 (1994).
32. A.S. Chen, Yu.M. Bunkov, H. Godfrin, R. Schanen, and F. Scheffer, *J. Low Temp. Phys.* **110**, 51 (1998).
33. A.S. Chen, Yu.M. Bunkov, H. Godfrin, R. Schanen, and F. Scheffer, *J. Low Temp. Phys.* **113**, 693 (1998).
34. D.J. Cousins, S.N. Fisher, A.I. Gregory, G.R. Pickett, and N.S. Shaw, *Phys. Rev. Lett.* **82**, 4484 (1999).
35. S. Autti, Yu.M. Bunkov, V.B. Eltsov, P.J. Heikkinen, J.J. Hosio, P. Hunger, M. Krusius, and G.E. Volovik, *Phys. Rev. Lett.* **108**, 145303 (2012).
36. Yu.M. Bunkov, O.D. Timofeevskaya, and G.E. Volovik, *Phys. Rev. Lett.* **73**, 1817 (1994).
37. Yu.M. Bunkov, V.S. L'vov, and G.E. Volovik, *JETP Lett.* **84**, 289 (2006).
38. Yu.M. Bunkov, E. Collin, and H. Godfrin, *J. Phys. Chem. Solids* **66**, 1325 (2005).

39. W.P. Halperin, H. Choi, J.P. Davis, and J. Pollanen, *J. Phys. Soc. Jpn.* **77**, 111002 (2008).
40. V.V. Dmitriev, V.V. Zavjalov, D.E. Zmeev, I.V. Kosarev, and N. Mulders, *JETP Lett.* **76**, 321 (2002).
41. Yu.M. Bunkov, E. Collin, H. Godfrin, and R. Harakaly, *Physica B* **329**, 305 (2003).
42. T. Kunimatsu, A. Matsubara, K. Izumina, T. Sato, M. Kubota, T. Takagi, Yu.M. Bunkov, and T. Mizusaki, *J. Low Temp. Phys.* **150**, 435 (2008).
43. P. Hunger, Yu.M. Bunkov, E. Collin, and H. Godfrin, *J. Low Temp. Phys.* **158**, 129 (2010).
44. T. Sato, T. Kunimatsu, K. Izumina, A. Matsubara, M. Kubota, T. Mizusaki, and Yu.M. Bunkov, *Phys. Rev. Lett.* **101**, 055301 (2008).
45. P.G. De Gennes, P.A. Pinkus, F. Hartmann-Boutron, and J.M. Winter, *Phys. Rev.* **129**, 1105 (1963); *J. Appl. Phys.* **34**, 1036 (1964).
46. M.S. Tagirov, E.M. Alakshin, Yu.M. Bunkov, R.R. Gazizulin, A.M. Gazizulina, L.I. Isaenko, A.V. Klochkov, T.R. Safin, K.R. Safiullin, and S.A. Zhurkov, *J. Low Temp. Phys.* **175**, 167 (2014).
47. V.A. Tulin, *Sov. Phys. JETP* **28**, 431 (1969).
48. M.I. Kurkin, *JETP Lett.* **28**, 675 (1978).